J|A|C|S ARTICLES

Published on Web 10/27/2010

Design, Synthesis, and Operation of Small Molecules That Walk along Tracks

Max von Delius, Edzard M. Geertsema, David A. Leigh,* and Dan-Tam D. Tang

School of Chemistry, University of Edinburgh, The King's Buildings, West Mains Road, Edinburgh EH9 3JJ, United Kingdom

Received July 22, 2010; E-mail: david.leigh@ed.ac.uk

Abstract: The synthesis and system dynamics of a series of small-molecule walker-track conjugates, 3,4-$\mathbf{C}_n$ (n = 2, 3, 4, 5, and 8), based on dynamic covalent linkages between the "feet" of the walkers and the "footholds" of the track, is described. Each walker has one acyl hydrazide and one sulfur-based foot separated by a spacer chain of "n" methylene groups, while the track consists of four footholds of alternating complementary functionalities (aldehydes and masked thiols). Upon repeatedly switching between acid and base, the walker moiety can be exchanged between the footholds on the track, primarily through a "passing-leg gait" mechanism, until a steady state, minimum energy, distribution is reached. The introduction of a kinetically controlled step in the reaction sequence (redox-mediated breaking and reforming of the disulfide linkages) can cause a directional bias in the distribution of the walker on the track. The different length walker molecules exhibit very different walking behaviors: Systems n = 2 and 3 cannot actually "walk" along the track because their stride lengths are too short to bridge the internal footholds. The walkers with longer spacers (n = 4, 5, and 8) do step up and down the track repeatedly, but a directional bias under the acid−redox conditions is only achieved for the $\mathbf{C_4}$ and $\mathbf{C_5}$ systems, interestingly in opposite directions (the $\mathbf{C_8}$ walker has insufficient ring strain with the track). Although they are extremely rudimentary systems, the $\mathbf{C_4}$ and $\mathbf{C_5}$ walker−track conjugates exhibit four of the essential characteristics of linear molecular motor dynamics: processive, directional, repetitive, and progressive migration of a molecular unit up and down a molecular track.

Introduction

Although many biological processes utilize molecules that convert chemical energy into directed molecular level motion,[1] most of the artificial molecular machines prepared to date only do so to a very limited degree.[2,3] For example, rotaxanes have been developed that can change the relative positions of their components to collectively cause the transport of liquid droplets up a slope against the force of gravity[4] or to bend cantilevers.[5] However, such systems cannot act progressively; that is, they cannot be reset to do further mechanical work on a system without undoing the task they originally performed, and so are best considered molecular switches, not motors.[2] Synthetic molecules that behave as rotary motors have been developed, working either through the sequential application of stimuli[3a,c,e,g] or at a constant photostationary state.[3b,f,i,k,n] Linear molecular motors are widely used to carry out mechanical work in biology, moving down tracks, transporting cargo, progressively exerting force, and performing many other tasks.[1] There are currently no synthetic small-molecule systems that can carry out such functions, and so we have embarked on a program to pursue these goals, starting with the design and construction of artificial molecules that can be transported progressively and directionally, without detaching, along a molecular track. Here, we report on the synthesis and behavior under operating conditions of a series of small-molecule walker−track conjugates, 3,4-$\mathbf{C}_n$ (n = 2, 3, 4, 5, and 8), based on dynamic covalent linkages between the "feet" of the walkers and the "footholds" of the track. The

(1) *Molecular Motors*; Schliwa, M., Ed.; Wiley-VCH: Weinheim, Germany, 2003.
(2) Kay, E. R.; Leigh, D. A.; Zerbetto, F. *Angew. Chem., Int. Ed.* **2007**, *46*, 72–191.
(3) (a) Kelly, T. R.; De Silva, H.; Silva, R. A. *Nature* **1999**, *401*, 150–152. (b) Koumura, N.; Zijlstra, R. W. J.; van Delden, R. A.; Harada, N.; Feringa, B. L. *Nature* **1999**, *401*, 152–155. (c) Leigh, D. A.; Wong, J. K. Y.; Dehez, F.; Zerbetto, F. *Nature* **2003**, *424*, 174–179. (d) Thordarson, P.; Bijsterveld, E. J. A.; Rowan, A. E.; Nolte, R. J. M. *Nature* **2003**, *424*, 915–918. (e) Hernandez, J. V.; Kay, E. R.; Leigh, D. A. *Science* **2004**, *306*, 1532–1537. (f) van Delden, R. A.; ter Wiel, M. K. J.; Pollard, M. M.; Vicario, J.; Koumura, N.; Feringa, B. L. *Nature* **2005**, *437*, 1337–1340. (g) Fletcher, S. P.; Dumur, F.; Pollard, M. M.; Feringa, B. L. *Science* **2005**, *310*, 80–82. (h) Balzani, V.; Clemente-León, M.; Credi, A.; Ferrer, B.; Venturi, M.; Flood, A. H.; Stoddart, J. F. *Proc. Natl. Acad. Sci. U.S.A.* **2006**, *103*, 1178–1183. (i) Eelkema, R.; Pollard, M. M.; Vicario, J.; Katsonis, N.; Serrano Ramon, B.; Bastiaansen, C. W. M.; Broer, D. J.; Feringa, B. L. *Nature* **2006**, *440*, 163. (j) Muraoka, T.; Kinbara, K.; Aida, T. *Nature* **2006**, *440*, 512–515. (k) Pijper, D.; Feringa, B. L. *Angew. Chem., Int. Ed.* **2007**, *46*, 3693–3696. (l) Serreli, V.; Lee, C.-F.; Kay, E. R.; Leigh, D. A. *Nature* **2007**, *445*, 523–527. (m) Alvarez-Pérez, M.; Goldup, S. M.; Leigh, D. A.; Slawin, A. M. Z. *J. Am. Chem. Soc.* **2008**, *130*, 1836–1838. (n) Klok, M.; Boyle, N.; Pryce, M. T.; Meetsma, A.; Browne, W. R.; Feringa, B. L. *J. Am. Chem. Soc.* **2008**, *130*, 10484–10485. (o) Panman, M. R.; Bodis, P.; Shaw, D. J.; Bakker, B. H.; Newton, A. C.; Kay, E. R.; Brouwer, A. M.; Buma, W. J.; Leigh, D. A.; Woutersen, S. *Science* **2010**, *328*, 1255–1258.
(4) Berná, J.; Leigh, D. A.; Lubomska, M.; Mendoza, S. M.; Pérez, E. M.; Rudolf, P.; Teobaldi, G.; Zerbetto, F. *Nat. Mater.* **2005**, *4*, 704–710.
(5) Huang, T. J.; Brough, B.; Ho, C.-M.; Liu, Y.; Flood, A. H.; Bonvallet, P. A.; Tseng, H.-R.; Stoddart, J. F.; Baller, M.; Magonov, S. *Appl. Phys. Lett.* **2004**, *85*, 5391–5393.

10.1021/ja106486b

synthesis and some of the properties of the C_5 system were recently reported in a preliminary communication.[6]

Molecules That Walk along Tracks. Spectacular examples of biological linear molecular motors include the kinesin, myosin, and dynein bipedal motor proteins, which are directionally driven along intracellular tracks by adenosine triphosphate (ATP) hydrolysis.[7] The main features[8,9] of biological linear molecular motor dynamics are processivity, directionality, and repetitive, progressive, and autonomous operation.

(i) Processivity is the ability of the molecular motor to remain attached to its track while it is directionally transported, that is, without detaching or exchanging with other molecules in the bulk.[10] Most wild-type kinesins exhibit a relatively high level of processivity, falling off their microtubular[11] tracks after an average of ~100 steps.[12]

(ii) Directionality is the tendency of a molecular walker to migrate preferentially toward a particular end of a polymeric track. Most kinesins show near-perfect directionality,[8] moving toward the plus-end of microtubules as long as the chemical potential of ATP is greater than that of adenosine diphosphate (ADP) and inorganic phosphate (P_i).[13] However, some kinesins, such as KIF1A,[14] only migrate with modest net directionality; that is, they take almost as many steps in the backward direction as they do in the forward direction. This type of dynamics has been described as "biased Brownian movement" or "diffusion with a drift".[15]

(iii) Repetitive operation is the motor's ability to repeatedly perform similar mechanical cycles. Kinesin takes one 8 nm step, putting one foot in front of the other, and each time an ATP molecule is hydrolyzed by the protein.[8]

(iv) Progressive operation is the ability of the molecular motor to be reset at the end of each mechanical cycle without undoing the physical task that was originally performed. The two feet of kinesin are identical, and yet it selectively moves first one foot and then the other in a passing-leg gait to transport itself continuously in the same direction along the track.[8]

(v) Autonomous operation is the ability of the molecular motor to undergo directional, processive motion as long as a chemical "fuel" is present, that is, without further external intervention (such as the application of a sequence of stimuli).

Features i−iv are key requirements for most types of molecular motor.[10] Autonomous operation, (v), can be an additional desirable trait but could also result in reduced control over a system; for example, it may not be possible to control the speed or distance traveled by a walker, nor to stop it unless and until the "fuel" runs out or the system is "clocked". Autonomous operation also implies that walker transport is only possible in one direction with a given fuel, a feature of biological motors but not necessarily a constraint that synthetic systems must adhere to. Our initial aim was to learn how to construct and operate synthetic small molecules that possess some of these key features of linear molecular motor dynamics. Until recently,[6] the only synthetic molecular structures that had been shown to exhibit most of these features were systems constructed from DNA.[16] Small-molecule walkers that do not utilize building blocks taken from biology are more fundamental systems that could offer advantages in terms of size, function, and modes of operation.

(6) (a) von Delius, M.; Geertsema, E. M.; Leigh, D. A. *Nat. Chem.* **2010**, *2*, 96–101. (b) Otto, S. *Nat. Chem.* **2010**, *2*, 75–76.

(7) For excellent concise reviews of the kinesin, myosin, and dynein linear motor families, see: (a) Vale, R. D. *Cell* **2003**, *112*, 467–480. (b) Schliwa, M.; Woehlke, G. *Nature* **2003**, *422*, 759–765.

(8) For reviews on kinesin, see: (a) Woehlke, G.; Schliwa, M. *Nat. Rev. Mol. Cell Biol.* **2000**, *1*, 50–58. (b) Asbury, C. L. *Curr. Opin. Cell Biol.* **2005**, *17*, 89–97. (c) Carter, N. J.; Cross, R. A. *Curr. Opin. Cell Biol.* **2006**, *18*, 61–67. (d) Block, S. M. *Biophys. J.* **2007**, *92*, 2986–2995.

(9) (a) Gilbert, S. P.; Webb, M. R.; Brune, M.; Johnson, K. A. *Nature* **1995**, *373*, 671–676. (b) Kull, F. J.; Sablin, P. S.; Lau, R.; Fletterick, R. J.; Vale, R. D. *Nature* **1996**, *380*, 550–555. (c) Schnitzer, M. J.; Block, S. M. *Nature* **1997**, *388*, 386–390. (d) Hua, W.; Chung, J.; Gelles, J. *Science* **2002**, *295*, 844–848. (e) Naber, N.; Minehardt, T. J.; Rice, S.; Chen, X.; Grammer, J.; Matuska, M.; Vale, R. D.; Kollman, P. A.; Car, R.; Yount, R. G.; Cooke, R.; Pate, E. *Science* **2003**, *300*, 798–801. (f) Asbury, C. L.; Fehr, A. N.; Block, S. M. *Science* **2003**, *302*, 2130–2134. (g) Yildiz, A.; Tomishige, M.; Vale, R. D.; Selvin, P. R. *Science* **2004**, *303*, 676–678. (h) Carter, N. J.; Cross, R. A. *Nature* **2005**, *435*, 308–312. (i) Shao, Q.; Gao, Y. Q. *Proc. Natl. Acad. Sci. U.S.A.* **2006**, *103*, 8072–8077. (j) Shao, Q.; Gao, Y. Q. *Biochemistry* **2007**, *46*, 9098–9106. (k) Alonso, M. C.; Drummond, D. R.; Kain, S.; Hoeng, J.; Amos, L.; Cross, R. A. *Science* **2007**, *316*, 120–123. (l) Mori, T.; Vale, R. D.; Tomishige, M. *Nature* **2007**, *450*, 750–754. (m) Guydosh, N. R.; Block, S. M. *Nature* **2009**, *461*, 125–128.

(10) Most motors from the myosin family do not operate processively. The processivity of dyneins depends on the concentration of ATP (see ref 7b).

(11) (a) Hirose, K.; Löwe, J.; Alonso, M.; Cross, R. A.; Amos, L. A. *Cell Struct. Funct.* **1999**, *24*, 277–284. (b) Kozielski, F.; Arnal, I.; Wade, R. H. *Curr. Biol.* **1998**, *8*, 191–198. (c) Marx, A.; Müller, J.; Mandelkow, E.-M.; Hoenger, A.; Mandelkow, E. *J. Muscle Res. Cell Motil.* **2006**, *27*, 125–137.

(12) (a) Howard, J.; Hudspeth, A. J.; Vale, R. D. *Nature* **1989**, *342*, 154–158. (b) Block, S. M.; Goldstein, L. S. B.; Schnapp, B. J. *Nature* **1990**, *348*, 348–352. (c) Hackney, D. D. *Nature* **1995**, *377*, 448–450. (d) Vale, R. D.; Funatsu, T.; Pierce, D. W.; Romberg, L.; Harada, Y.; Yanagida, T. *Nature* **1996**, *380*, 451–453. (e) Case, R. B.; Pierce, D. W.; Hom-Booher, N.; Hart, C. L.; Vale, R. D. *Cell* **1997**, *90*, 959–966. (f) Romberg, L.; Pierce, D. W.; Vale, R. D. *J. Cell Biol.* **1998**, *140*, 1407–1416. (g) Thorn, K. S.; Ubersax, J. A.; Vale, R. D. *J. Cell Biol.* **2000**, *151*, 1093–1100. (h) Yajima, J.; Alonso, M. C.; Cross, R. A.; Toyoshima, Y. Y. *Curr. Biol.* **2002**, *12*, 301–306.

(13) (a) Astumian, R. D. *Phys. Chem. Chem. Phys.* **2007**, *9*, 5067–5083. (b) Astumian, R. D.; Derényi, I. *Eur. Biophys. J.* **1998**, *27*, 474–489. (c) Astumian, R. D. *Biophys. J.* **2010**, *98*, 2401–2409.

(14) Hirokawa, N.; Nitta, R.; Okada, Y. *Nat. Rev. Mol. Cell Biol.* **2009**, *10*, 877–884.

(15) Okada, Y.; Hirokawa, N. *Science* **1999**, *283*, 1152–1157.

(16) (a) Sherman, W. B.; Seeman, N. C. *Nano Lett.* **2004**, *4*, 1203–1207. (b) Shin, J.-S.; Pierce, N. A. *J. Am. Chem. Soc.* **2004**, *126*, 10834–10835. (c) Yin, P.; Yan, H.; Daniell, X. G.; Turberfield, A. J.; Reif, J. H. *Angew. Chem., Int. Ed.* **2004**, *43*, 4906–4911. (d) Tian, Y.; He, Y.; Chen, Y.; Yin, P.; Mao, C. *Angew. Chem., Int. Ed.* **2005**, *44*, 4355–4358. (e) Pei, R.; Taylor, S. K.; Stefanovic, D.; Rudchenko, S.; Mitchell, T. E.; Stojanovic, M. N. *J. Am. Chem. Soc.* **2006**, *128*, 12693–1269. (f) Yin, P.; Choi, H. M. T.; Calvert, C. R.; Pierce, N. A. *Nature* **2008**, *451*, 318–322. (g) Green, S. J.; Bath, J.; Turberfield, A. J. *Phys. Rev. Lett.* **2008**, *101*, 238101. (h) Omabegho, T.; Sha, R.; Seeman, N. C. *Science* **2009**, *324*, 67–71. (i) Gu, H.; Chao, J.; Xiao, S.-J.; Seeman, N. C. *Nature* **2010**, *465*, 202–205. (j) Lund, K.; Manzo, A. J.; Dabby, N.; Michelotti, N.; Johnson-Buck, A.; Nangreave, J.; Taylor, S.; Pei, R.; Stojanovic, M. N.; Walter, N. G.; Winfree, E.; Yan, H. *Nature* **2010**, *465*, 206–210.

(17) In some cases (e.g., the Payne rearrangement), only bonds, rather than molecular fragments, migrate. In others, such as the Cope rearrangement, the migration of atoms proceeds processively (i.e., intramolecularly). However, such migrations are generally neither repetitive, nor progressive (the 1,4-Cope rearrangement of an allyl ether can occur twice in a row if the 2-position is blocked: Ryan, J. P.; O'Connor, P. R. *J. Am. Chem. Soc.* **1952**, *74*, 5866−5869). Metal complexes often migrate around ring systems and along other molecular frameworks, for example: Strawser, D.; Karton, A.; Zenkina, O. V.; Iron, M. A.; Shimon, L. J. W.; Martin, J. M. L.; van der Boom, M. E. *J. Am. Chem. Soc.* **2005**, *127*, 9322–9323, but not directionally in a sense that can be repetitively propagated. In other reactions, for example, the exchange of acetals between the hydroxyl groups of carbohydrates, the migration of the molecular fragments is an intrinsically nondirectional and non-processive process (intramolecular exchange competes with exchange with the bulk). For details of these, and other examples of rearrangements, see: Kürti, L.; Czakó, B. *Strategic Applications of Named Reactions*; Elsevier: Oxford, UK, 2005; and references cited therein.

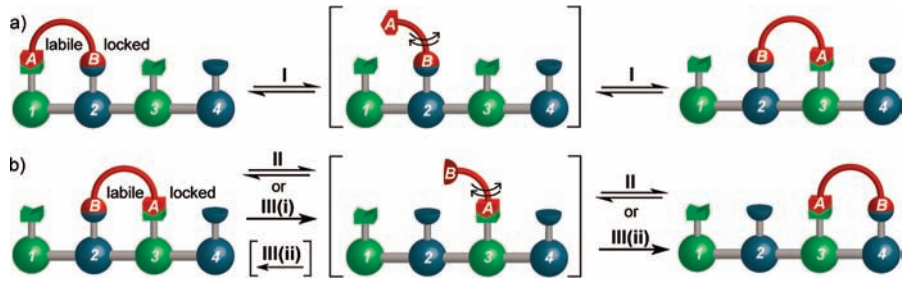

Figure 1. Graphical representation of processive migration of a two-legged "walker" molecule (red) along a track featuring two different possible binding sites (green and blue) for the two chemically different feet. Two key intermediate states, in which one or the other foot is disconnected from the track, are shown in square brackets. For the walking action to be processive, the two feet of the walker (labeled "A" and "B") must never be disconnected from the track at the same time. In chemical terms, the way that this is achieved in this system is that the foot−track bond disconnections (I and either II or III) are designed to occur under mutually exclusive sets of conditions.

Design of a Synthetic Small-Molecule Walker. Although there are many chemical reactions that feature the migration of molecular fragments, few appear well-suited for developing into a processive, directional, and repetitive motor mechanism.[17] There are, however, some reports of small molecular units that move processively (i.e., without detaching) along molecular frameworks. Lawton and co-workers have described a series of reagents for the cross-linking of biomolecules under thermodynamic control.[18] These molecules are transferred between accessible nucleophilic (amine and thiol) sites on proteins such as ribonuclease.[16a] The transport proceeds intramolecularly (i.e., processively) due to the clever construction of the cross-linking moiety: only one or two, never zero, of the nucleophilic footholds are attached to the cross-linking molecule at any one time as it is passed from one nucleophilic site to another intramolecularly toward the thermodynamic minimum.[19] During polymer synthesis, catalytic metal species have been shown to migrate intramolecularly for considerable distances along polymer chains growing by Kumada catalyst-transfer polycondensation[20] and during ethylene polymerization.[21] Finally, Schalley and co-workers have described systems in which crown ethers apparently migrate processively along linear or cyclic molecular scaffolds under the extreme dilution conditions present in the high vacuum of a FTICR mass spectrometer.[22]

Our approach to a bipedal small molecule that can walk down a molecular track is outlined in Figure 1. The walker unit (shown in red) is intended to traverse the track by a "passing-leg" gait involving two chemically different "feet" ("A" and "B") that reversibly bind to different regions of the track. Linear motor proteins and the synthetic DNA walkers use noncovalent interactions for track binding, but the understanding of how to sequentially kinetically lock and release different artificial hydrogen bond (for example) recognition sites in the desired manner is beyond the capabilities of present day synthetic supramolecular chemistry. We instead chose to utilize dynamic covalent chemistry[23] for this purpose, which combines some of the features of supramolecular chemistry (reversibility, dynamics) with those of covalent bond chemistry (bond strength, robustness). To prevent the walker from completely detaching from the track during the walking process, the different feet form covalent bonds that are labile or kinetically locked under mutually exclusive sets of conditions.[24] Under condition I (Figure 1a), foot "A" can dissociate from the track, while the bond between foot "B" and the track is kinetically locked. Under conditions II or III (Figure 1b), the situation is reversed. This unusual property of the system confers processivity on the walking process.

Results and Discussion

Synthesis. The construction of walker−track conjugate 1,2-$\mathbf{C_5}$, in which the molecular walker is attached to a four-foothold track via hydrazone (labile in acid; locked in base) and disulfide (labile in base; locked in acid) linkages,[24b−d] is shown in Scheme 1.[6] Acyl hydrazones were chosen for the acid-labile linkage rather than imines as they are generally more kinetically inert under neutral or basic conditions and when isolated.[25] Benzylic thiols were utilized on the track, because they can be introduced under mild conditions at a late stage of the synthesis.

Building blocks **1**−**4** were synthesized according to published procedures.[26] Williamson ether synthesis (steps i and vii), mesylation (steps ii and viii), and nucleophilic substitution with potassium thioacetate (steps iii and ix) generated the key two-

(18) (a) Mitra, S.; Lawton, R. G. *J. Am. Chem. Soc.* **1979**, *101*, 3097–3110. (b) Liberatore, F. A.; Comeau, R. D.; McKearin, J. M.; Pearson, D. A.; Belonga, B. Q.; Brocchini, S. J.; Kath, J.; Phillips, T.; Oswell, K.; Lawton, R. G. *Bioconjugate Chem.* **1990**, *1*, 36–50. (c) del Rosario, R. B.; Brocchini, S. J.; Lawton, R. G.; Wahl, R. L.; Smith, R. *Bioconjugate Chem.* **1990**, *1*, 50–58. (d) del Rosario, R. B.; Baron, L. A.; Lawton, R. G.; Wahl, R. L. *Nucl. Med. Biol.* **1992**, *19*, 417–421.

(19) Loss of processivity in these systems may occur through intermolecular bridges, the presence of which has been reported (ref 18a). Lawton and coworkers did not (and had no cause to) conduct studies on the processivity of their systems.

(20) Tkachov, R.; Senkovskyy, V.; Komber, H.; Sommer, J.-U.; Kiriy, A. *J. Am. Chem. Soc.* **2010**, *132*, 7803–7810.

(21) (a) Johnson, L. K.; Killian, C. M.; Brookhart, M. *J. Am. Chem. Soc.* **1995**, *117*, 6414–6415. (b) Möhring, M.; Fink, G. *Angew. Chem., Int. Ed. Engl.* **1985**, *24*, 1001–1002.

(22) (a) Winkler, H. D. F.; Weimann, D. P.; Springer, A.; Schalley, C. A. *Angew. Chem., Int. Ed.* **2009**, *48*, 7246–7250. (b) Weimann, D. P.; Winkler, H. D. F.; Falenski, J. A.; Koksch, B.; Schalley, C. A. *Nat. Chem.* **2009**, *1*, 573–577.

(23) (a) Rowan, S. J.; Cantrill, S. J.; Cousins, G. R. L.; Sanders, J. K. M.; Stoddart, J. F. *Angew. Chem., Int. Ed.* **2002**, *41*, 898–952. (b) Corbett, P. T.; Leclaire, J.; Vial, L.; West, K. R.; Wietor, J.-L.; Sanders, J. K. M.; Otto, S. *Chem. Rev.* **2006**, *106*, 3652–3711. (c) Lehn, J.-M. *Chem. Soc. Rev.* **2007**, *36*, 151–160.

(24) (a) Goral, V.; Nelen, M. I.; Eliseev, A. V.; Lehn, J.-M. *Proc. Natl. Acad. Sci. U.S.A.* **2001**, *98*, 1347–1352. (b) Orrillo, A. G.; Escalante, A. M.; Furlan, R. L. E. *Chem. Commun.* **2008**, 5298–5300. (c) Rodriguez-Docampo, Z.; Otto, S. *Chem. Commun.* **2008**, 5301–5303. (d) von Delius, M.; Geertsema, E. M.; Leigh, D. A.; Slawin, A. M. Z. *Org. Biomol. Chem.* **2010**, *8*, 4617−4624.

(25) For an example where unstable imines are reduced to stable secondary amines, see: Hochgurtel, M.; Kroth, H.; Piecha, D.; Hofmann, M. W.; Nicolaou, K. C.; Krause, S.; Schaaf, O.; Sonnenmoser, G.; Eliseev, A. V. *Proc. Natl. Acad. Sci. U.S.A.* **2002**, *99*, 3382–3387.

(26) (a) Costioli, M. D.; Berdat, D.; Freitag, R.; André, X.; Müller, A. H. E. *Macromolecules* **2005**, *38*, 3630–3637. (b) Lin, D.; Zhang, J.; Sayre, L. M. *J. Org. Chem.* **2007**, *72*, 9471–9480. (c) Klein, L. L.; Yeung, C. M.; Kurath, P.; Mao, J. C.; Fernandes, P. B.; Lartey, P. A.; Pernet, A. G. *J. Med. Chem.* **1989**, *32*, 151–160.

Scheme 1. (a) Synthesis of Walker−Track Conjugate 1,2-$\mathbf{C_5}$,[a] (b) General Structure of Walker−Track Conjugates 3,4-$\mathbf{C_n}$, and (c) 3,4-$\mathbf{C_5}$-d_4, a Walker−Track System Deuterium-Labeled on Both the Walker and the Track Units

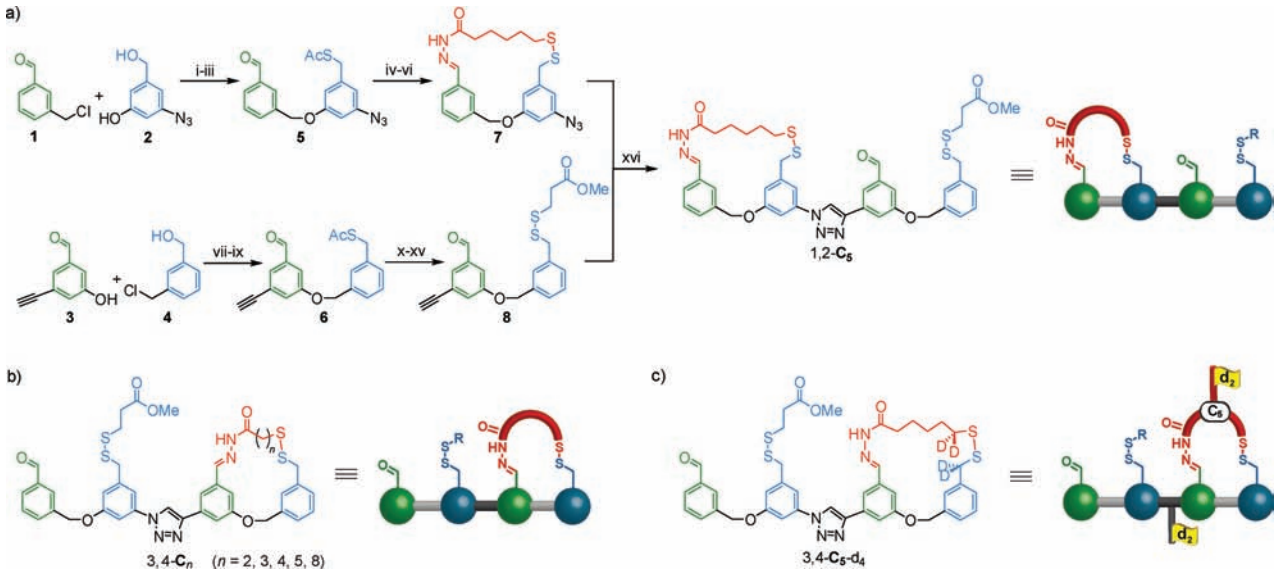

[a] (i) NaH, dimethylformamide (DMF), room temperature, 16 h, 88%; (ii) methanesulfonyl chloride (MsCl), Et_3N, CH_2Cl_2, 0 °C, 30 min; (iii) KSAc, DMF, room temperature, 3 h, 77% (over two steps); (iv) 6-mercaptohexanoic acid hydrazide, AcOH (cat.), MeOH, room temperature, 2 h, 78%; (v) NaOMe, MeOH, room temperature, 2 h; (vi) I_2, KI, CH_2Cl_2, room temperature, 5 min, 32% (over two steps); (vii) NaH, DMF, 0 °C to room temperature, 16 h, 65%; (viii) MsCl, Et_3N, CH_2Cl_2, room temperature, 16 h; (ix) KSAc, DMF, room temperature, 3 h, 66% (over two steps); (x) $HC(OMe)_3$, *p*-toluenesulfonic acid (*p*-TsOH), MeOH, room temperature, 30 min; (xi) NaOMe, MeOH, room temperature, 30 min; (xii) 3-mercaptopropionic acid, I_2, KI, CH_2Cl_2, room temperature, 5 min; (xiii) trifluoroacetic acid (TFA), CH_2Cl_2, room temperature, 30 min, 58% (over four steps); (xiv) H_2SO_4 (cat.), MeOH, room temperature, 16 h; (xv) TFA, CH_2Cl_2, room temperature, 30 min, 40% (over two steps); (xvi) $Cu(MeCN)_4PF_6$, tris[(1-benzyl-1*H*-1,2,3-triazol-4-yl)methyl]amine (TBTA), CH_2Cl_2/tetrahydrofuran (THF)/MeOH, room temperature, 16 h, 79%.

foothold precursors **5** and **6**. The starting position of the walker at footholds 1 and 2 in the walker−track conjugate was established by synthesizing macrocycle **7** by acid-catalyzed condensation (step iv) of aldehyde **5** to the bifunctional walker compound 6-mercaptohexanoic acid hydrazide, subsequent thioacetate methanolysis (step v), and oxidative ring closure (step vi). The sulfur foothold of the track (e.g., foothold 4 in 1,2-$\mathbf{C_5}$) was protected as a disulfide (using a "placeholder" thiol; see Scheme 1a), to prevent atmospheric oxygen oxidizing the free thiol to a dimeric disulfide. To achieve this, an unsymmetric disulfide bond (see compound **8** in Scheme 1a) had to be constructed, which was achieved through oxidation of the track thiol in the presence of an excess of the placeholder thiol (step xii). Finally, a ligand-assisted copper(I)-catalyzed alkyne−azide cycloaddition (CuAAC)[27] was used to couple macrocycle **7** to the building block (**8**) containing footholds 3 and 4 (Scheme 1a, step xvi). The CuAAC reaction has excellent functional group compatibility and introduces a rigid triazole linkage into the molecular track, which reduces the tendency for track folding.

Positional isomer 3,4-$\mathbf{C_5}$ (Scheme 1b), in which the walker unit is located at the other end of the track, was prepared unambiguously from **5** and **6** following analogous synthetic procedures,[6] together with a series of walker moieties differing in the number (2, 3, 4, and 8) of methylene groups between the functional group "feet". The various walker units were condensed with aldehyde **6** and subsequently converted to walker−track conjugates 3,4-$\mathbf{C_2}$, 3,4-$\mathbf{C_3}$, 3,4-$\mathbf{C_4}$, and 3,4-$\mathbf{C_8}$[28] (see the Supporting Information for synthetic procedures and characterization data). Finally, an analogue of 3,4-$\mathbf{C_5}$ was prepared that was deuterium-labeled on both the walker unit and the track (3,4-$\mathbf{C_5}$-d_4, Scheme 1c) to investigate the processivity of the walking dynamics (vide infra).

Hydrazone Exchange and Disulfide Exchange under Thermodynamic Control (Walking with No Directional Bias). We initially investigated the change of position of the various walker units on the track under conditions for reversible (dynamic) covalent bond exchange (Scheme 2). Dilute solutions of 1,2-$\mathbf{C_5}$ were subjected to acidic conditions typically used[29] for hydrazone exchange (Scheme 2, conditions I), whereas solutions of 3,4-$\mathbf{C_5}$ were subjected to basic conditions typically used[30] for

(27) (a) Chan, T. R.; Hilgraf, R.; Sharpless, K. B.; Fokin, V. V. *Org. Lett.* **2004**, *17*, 2853–2855. (b) Fokin, V. V.; Wu, P. *Aldrichimica Acta* **2007**, *40*, 7–17. (c) Lee, B.-Y.; Park, S. R.; Jeon, H. B.; Kim, K. S. *Tetrahedron Lett.* **2006**, *47*, 5105–5109.

(28) We use the abbreviation $\mathbf{C_n}$ to indicate the whole series of walker−track conjugates (*n* corresponds to the number of methylene units in the spacer chain of the walker moiety).

(29) For examples of hydrazone exchange in organic solvents, see: (a) Cousins, G. R. L.; Poulsen, S. A.; Sanders, J. K. M. *Chem. Commun.* **1999**, 1575–1576. (b) Furlan, R. L. E.; Cousins, G. R. L.; Sanders, J. K. M. *Chem. Commun.* **2000**, 1761–1762. (c) Cousins, G. R. L.; Furlan, R. L. E.; Ng, Y.-F.; Redman, J. E.; Sanders, J. K. M. *Angew. Chem., Int. Ed.* **2001**, *40*, 423–426. (d) Furlan, R. L. E.; Ng, Y.-F.; Otto, S.; Sanders, J. K. M. *J. Am. Chem. Soc.* **2001**, *123*, 8876–8877. (e) Furlan, R. L. E.; Ng, Y.-F.; Cousins, G. R. L.; Redman, J. E.; Sanders, J. K. M. *Tetrahedron* **2002**, *58*, 771–778. (f) Choudhary, S.; Morrow, J. R. *Angew. Chem., Int. Ed.* **2002**, *41*, 4096–4098. (g) Lam, T. S.; Belenguer, A.; Roberts, S. L.; Naumann, C.; Jarrosson, T.; Otto, S.; Sanders, J. K. M. *Science* **2005**, *308*, 667–669.

(30) For examples of disulfide exchange in organic solvents, see: (a) Hioki, H.; Still, W. C. *J. Org. Chem.* **1998**, *63*, 904–905. (b) Kieran, A. L.; Bond, A. D.; Belenguer, A. M.; Sanders, J. K. M. *Chem. Commun.* **2003**, 2674–2675. (c) ten Cate, A. T.; Dankers, P. Y. W.; Sijbesma, R. P.; Meijer, E. W. *J. Org. Chem.* **2005**, *70*, 5799. (d) Kieran, A. L.; Pascu, S. I.; Jarrosson, T.; Sanders, J. K. M. *Chem. Commun.* **2005**, 1276–1278. (e) Kieran, A. L.; Pascu, S. I.; Jarrosson, T.; Gunter, M. J.; Sanders, J. K. M. *Chem. Commun.* **2005**, 1842–1844. (f) Danieli, B.;

Scheme 2. Reversible Reactions That Connect Various Pairs of the Four Positional Isomers 1,2-$\mathbf{C}_n$, 2,3-$\mathbf{C}_n$, 3,4-$\mathbf{C}_n$, and 1,4-$\mathbf{C}_n$ under Conditions I or II[a]

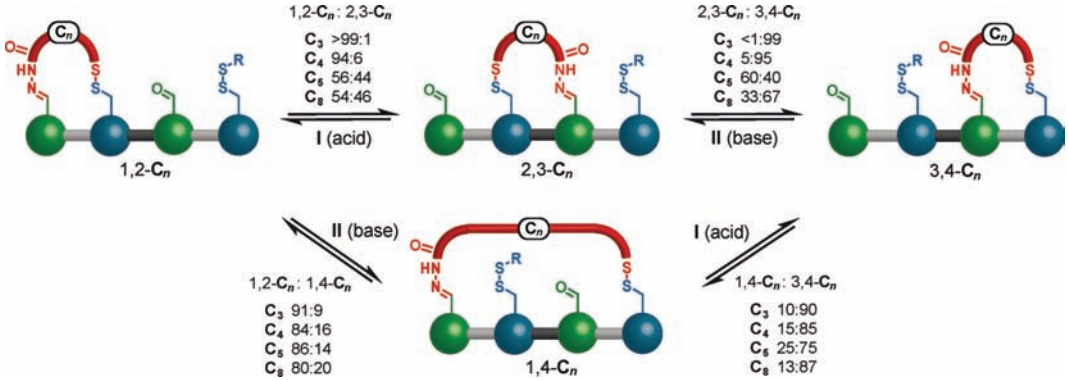

[a] Condition I (reversible hydrazone exchange): 0.1 mM, TFA, $CHCl_3$, room temperature, 6−96 h (monitored by HPLC until the distribution no longer changed). Condition II (reversible disulfide exchange): 0.1 mM, DTT (10 equiv), DBU (40 equiv), dimethyl 3,3′-disulfanediyldipropanoate (20 equiv), $CHCl_3$, room temperature, 12−48 h (monitored by HPLC until the distribution no longer changed).

disulfide exchange (Scheme 2, conditions II). In both cases, mixtures of the starting material together with positional (constitutional) isomer 2,3-$\mathbf{C}_5$ were obtained (Scheme 2).[31] Applying either set of conditions to a pristine sample of 2,3-$\mathbf{C}_5$[32] resulted in mixtures of identical composition, confirming that the dynamic exchange reactions were at chemical equilibrium.

Systematic optimization of the reaction parameters (see the Supporting Information for details) provided a set of conditions that led to equilibrium between each set of positional isomers in each walker system within a reasonable time period.[33] For hydrazone exchange[29] (e.g., exchange between the 1,2 and 2,3 isomers), adding trifluoroacetic acid (TFA) and a small amount of water (5% v/v with respect to TFA) to a solution (0.1 mM) of the walker−track conjugate in chloroform ($CHCl_3$) led to reliable and efficient conversion (no detectable amounts of oligomers or other side products) to a steady-state distribution of isomers. In the case of reversible disulfide exchange,[30] the optimized conditions utilized the same concentration (0.1 mM) of the walker−track conjugate in $CHCl_3$, a strong base (1,8-diazabicyclo[5.4.0]undec-7-ene (DBU)), a mild reducing agent (DL-dithiothreitol (DTT)), and dimethyl 3,3′-disulfanediyldipropanoate ($(MeO_2CCH_2CH_2S)_2$) as the placeholder disulfide.[34] To our surprise, subjecting 1,2-$\mathbf{C}_5$ to conditions for disulfide exchange (or 3,4-$\mathbf{C}_5$ to conditions for hydrazone exchange) also resulted in the formation of positional isomer 1,4-$\mathbf{C}_5$ (albeit in small relative amounts, 9−20%). We originally suspected this isomer would be too strained to be formed in appreciable quantities using reversible chemical reactions.

Scheme 2 shows the reversible reactions that connect various pairs of the four positional isomers 1,2-$\mathbf{C}_n$, 2,3-$\mathbf{C}_n$, 3,4-$\mathbf{C}_n$, and 1,4-$\mathbf{C}_n$ under conditions for hydrazone (I) and disulfide (II) exchange. In addition to the major passing-leg gait mechanism from 1,2-$\mathbf{C}_n$ to 3,4-$\mathbf{C}_n$ via 2,3-$\mathbf{C}_n$, 1,4-$\mathbf{C}_n$ provides a minor "double step" route from 1,2-$\mathbf{C}_n$ to 3,4-$\mathbf{C}_n$ (Scheme 2). It is interesting to note that occasional statistical "errors" to the major pathway mechanisms also occur with the working action of some biological motor proteins.[1,35]

We next quantified the position of equilibrium for every step of the walker migration under reversible conditions I and II for each set of walker−track conjugates ($\mathbf{C}_2$, $\mathbf{C}_3$, $\mathbf{C}_4$, $\mathbf{C}_5$, $\mathbf{C}_8$). In each case, the four sets of reactions that connect two pairs of positional isomers (1,2-$\mathbf{C}_n$:2,3-$\mathbf{C}_n$; 2,3-$\mathbf{C}_n$:3,4-$\mathbf{C}_n$; 1,2-$\mathbf{C}_n$:1,4-$\mathbf{C}_n$; 1,4-$\mathbf{C}_n$:3,4-$\mathbf{C}_n$) were investigated. For 3,4-$\mathbf{C}_4$, for example, the optimized conditions for disulfide exchange were applied, the equilibrium ratio between 3,4-$\mathbf{C}_4$ and 2,3-$\mathbf{C}_4$ was determined by HPLC (see the Supporting Information), and 2,3-$\mathbf{C}_4$ was subsequently isolated by semipreparative HPLC. With the pure sample of 2,3-$\mathbf{C}_4$ obtained from that experiment, two further experiments were performed: a reverse control reaction to equilibrate 2,3-$\mathbf{C}_4$ and 3,4-$\mathbf{C}_4$ and the hydrazone exchange reaction that results in equilibrium between 2,3-$\mathbf{C}_4$ and 1,2-$\mathbf{C}_4$. This procedure allowed the unambiguous determination of the equilibrium composition of every positional isomer pair, including the systems in which only the 3,4-isomer was initially prepared according to Scheme 1 ($\mathbf{C}_2$, $\mathbf{C}_3$, $\mathbf{C}_4$, and $\mathbf{C}_8$).

Scheme 2 summarizes the results of the quantitative studies on the steady-state composition of the reversible reaction between the various positional isomers (see the Supporting Information for examples of HPLC traces).[36] Three significant conclusions can be drawn from these results:

(i) The spacer length for the different walkers has a dramatic effect on the amount of 2,3-isomer that can be formed under the dynamic covalent bond exchange reactions. While 2,3-$\mathbf{C}_5$ is readily formed (44% from 1,2-$\mathbf{C}_5$ under acidic conditions and 60% from 3,4-$\mathbf{C}_5$ under basic conditions), 2,3-$\mathbf{C}_4$ is only formed in 5−6% yield, and 2,3-$\mathbf{C}_3$ is not detected at all.[37] This can be explained by a significant increase in ring strain with the smaller walkers. The net result is that the short "stride length" of these walkers limits their ability to walk down the molecular track. In effect, taking a step to the middle footholds becomes a rare event, and it requires many acid−base oscillations for a

Giardini, A.; Lesma, G.; Passarella, D.; Peretto, B.; Sacchetti, A.; Silvani, A.; Pratesi, G.; Zunino, F. *J. Org. Chem.* **2006**, *71*, 2848–2853.

(31) The structure of 2,3-$\mathbf{C}_5$ was confirmed by two-dimensional ^{1}H NMR spectroscopy (ROESY, COSY).[6] Further characterization involved high-resolution mass spectrometry, HPLC, and LCMS (see the Supporting Information).

(32) 2,3-$\mathbf{C}_5$ was isolated by preparative HPLC.[6]

(33) Disulfide exchange in organic solvents can require long periods of time to reach equilibrium. See refs 30c and 30f, where 20−120 days appear to be necessary.

(34) The placeholder disulfide is necessary to prevent oligomerization through disulfide bridges.

(35) Noji, H.; Yasuda, R.; Yoshida, M.; Kinosita, K. *Nature* **1997**, *386*, 299–302.

(36) The equilibria for the $\mathbf{C}_2$ system were not studied in detail as initial studies showed that the walker unit is too short to bridge the internal footholds to any significant degree.

(37) The HPLC detection limit is <1%.

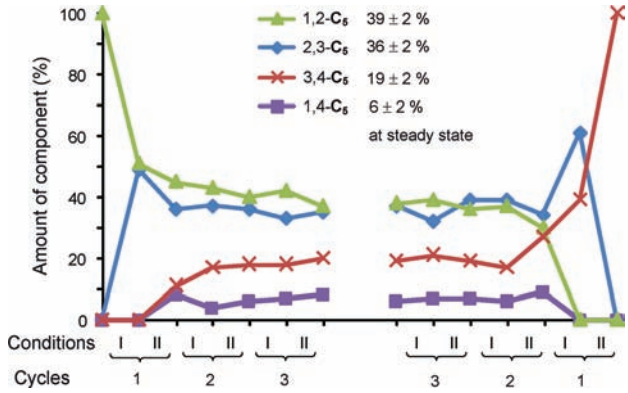

Figure 2. Product distribution during three cycles of directionally nonbiased, acid−base operation starting from pristine 1,2-$\mathbf{C}_5$ (left-hand side) and from pristine 3,4-$\mathbf{C}_5$ (right-hand side). Under each set of conditions (I and II), two different pairs of positional isomers are in equilibrium (see Scheme 2). Values are based on HPLC integration and are corrected for the absorbance coefficients at 290 nm (see the Supporting Information).

significant amount of these walkers to traverse the central footholds and thus move from one end of the track to the other.

(ii) The variation in spacer length of the walker unit has a marginal effect on the amount of 1,4-isomer formed (9−25%). In this positional isomer, the track forms a relatively large macrocycle with the walker. Making this large macrocycle smaller or larger by one atom has a negligible effect on ring strain and the relative free energy of the compound.

(iii) The equilibria between each "terminal" isomer (1,2 and 3,4) and the "internal" *2*,3 isomer do not consistently favor or disfavor the formation of the internal macrocycle (for example, with the $\mathbf{C}_5$ walker the 1,2-isomer is preferred over the 2,3-isomer, 1,2-$\mathbf{C}_5$:2,3-$\mathbf{C}_5$ (56:44), whereas the internal macrocycle is more thermodynamically stable than the 3,4-terminal isomer, 2,3-$\mathbf{C}_5$:3,4-$\mathbf{C}_5$ (60:40)).

For the $\mathbf{C}_5$ system, where all isomers were accessible in appreciable amounts (see Scheme 2), and where both the 1,2 and the 3,4 isomers were independently synthesized (Scheme 1), experiments that sequentially cycled between conditions I and II were conducted. Figure 2 (left-hand-side) shows how, starting from pristine 1,2-$\mathbf{C}_5$, switching between conditions I and II over several cycles leads to convergence of the positional isomer distribution to a ratio of 1,2-$\mathbf{C}_5$:2,3-$\mathbf{C}_5$:3,4-$\mathbf{C}_5$:1,4-$\mathbf{C}_5$ 39:36:19:6 (±2). A very similar distribution of positional isomers was obtained starting from pristine 3,4-$\mathbf{C}_5$ and carrying out the operation sequence over three cycles (Figure 2; right-hand side). Thus, irrespective of which end of the track the walker starts from, the effect of the "walking" operations is to reach the same steady-state positional distribution of the walker units on the track.

The behavior of the system raises the question if the observed steady-state distribution is minimizing free energy (in other words, if it corresponds to the lowest energy distribution for the walkers on the tracks). The answer to this question is not trivial, because under any one particular set of reaction conditions each of the four isomers can only exchange with the one positional isomer that it is "paired" with. The system can thus only move toward the thermodynamic minimum in a stepwise manner by switching back and forth between the different sets of conditions several times. Furthermore, in principle at least, the minimum energy distribution could be different under different sets of conditions (i.e., conditions I and II).

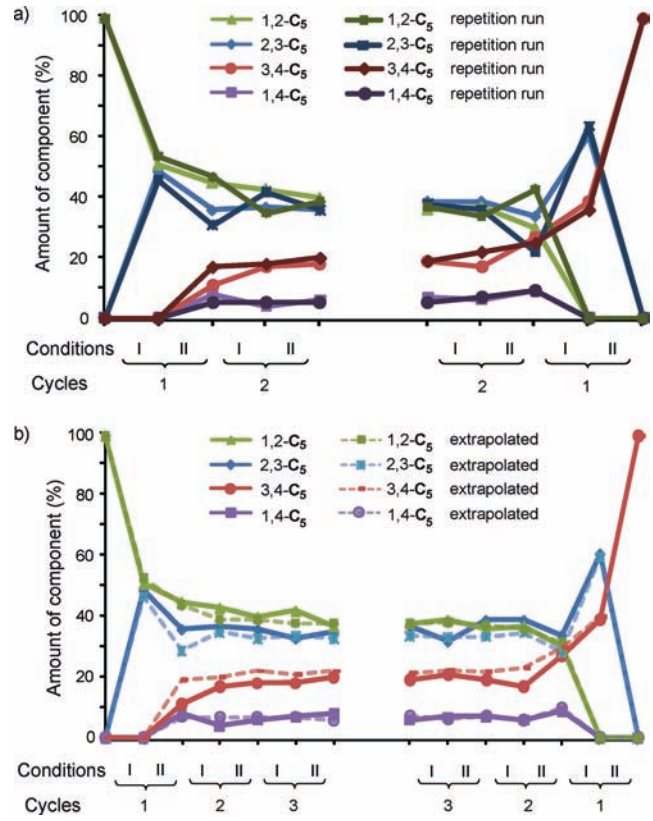

Figure 3. (a) Demonstration of the reproducibility of the experimental results from the operation of the $\mathbf{C}_5$ walker−track system and its "self-correcting" behavior. Product distribution during two cycles of directionally nonbiased, acid−base operation starting from pristine 1,2-$\mathbf{C}_5$ (left-hand side) and from pristine 3,4-$\mathbf{C}_5$ (right-hand side). The originally obtained data (lighter shade, identical to Figure 2) superimposed with data from a repetition run (darker shade). (b) Predictability of system evolution based on the equilibrium ratio of each pair of positional isomers. Product distribution during three cycles of directionally nonbiased, acid−base operation starting from pristine 1,2-$\mathbf{C}_5$ (left-hand side) and from pristine 3,4-$\mathbf{C}_5$ (right-hand side). Solid lines, first experimental series (identical to Figure 2); dashed lines, calculated data, based on extrapolation of the experimental ratios between each pair of positional isomers (see Scheme 2).

There is, however, compelling evidence that the steady-state distribution shown in Figure 2 does indeed correspond to the minimum energy of the system under both acidic and basic conditions:

(i) Once the system has reached the steady state (Figure 2), further oscillation of the conditions no longer changes (within experimental error) the composition of the mixture. In a situation where the relative energies of the positional isomers are different under conditions I and II, one would expect a graph that oscillates between two different steady states. This is not the case in Figure 2.

(ii) During the walking operations, the system moves to correct errors caused by imperfect experiments. Figure 3a shows a superimposition of the data from the original experimental data (from Figure 2) with data acquired during a repetition of the experimental sequence. Even though the isomer ratios differ slightly during some stages of the two experimental sequences (through normal variations and errors in the execution of the experiments; some reactions might not have gone to completion, sometimes the analysis might have errors, etc.), the final composition of positional isomers is the same in both experiments. The self-correcting nature of the system is an indication that the composition of the mixture always moves toward the minimum energy distribution.

Table 1. Steady-State Positional Isomer Distributions, Based on Experimentally Determined Multiple Cycles for C_5 and on Data Extrapolated from the Equilibrium between Each Pair of Positional Isomers for C_3, C_4, and C_8[a]

	C_3	C_4	C_5	C_8
1,2	52%	41%	39%	26%
2,3	<1%	3%	36%	22%
3,4	43%	48%	19%	45%
1,4	5%	8%	6%	7%
approx. number of cycles to converge	15	8	2	2

[a] See section 6 of the Supporting Information for graphs showing the evolution of the system (similar to the type of graphs used in Figures 2 and 3).

(iii) Figure 3b shows a superimposition of the original experimental data (solid lines) with theoretically calculated data (dashed lines) based on the extrapolation of the four experimentally determined equilibrium ratios between the individual pairs of positional isomers (see Scheme 2). Again, differences occur in the early cycles,[38] but the final composition of the mixture can be accurately predicted using only the four pairs of equilibrium ratios shown in Scheme 2. This demonstrates that the four equilibrium ratios between the pairs of positional isomers constitute a consistent set of relative energies that corresponds to the steady-state distribution.[39]

Having established that the composition of the system is determined only by the equilibrium between the four pairs of positional isomers and the number of cycles performed, analogous extrapolation calculations were performed for the C_3, C_4, and C_8 systems.[40] The resulting steady-state compositions are shown in Table 1 (see the Supporting Information for the extrapolation graphs). The minimum energy distributions of the walker units on the track are significant because they correspond to the distribution that a directionally biased walker must be transported away from.

Figure 4 shows a plot of the relative free energies of the positional isomers generated from the experimentally determined positional isomer ratios shown in Scheme 2. These relative energies only refer to the particular experimental conditions used in Scheme 2, but, nevertheless, provide a qualitative basis for understanding the observed isomer ratios and a rationale for the behavior of the different length walker units under operating conditions that could bias the directionality of walker migration (vide infra).

From Nondirectional Walker Migration to Directional Walker Transport (Hydrazone Exchange under Thermodynamic Control; Disulfide Exchange under Kinetic Control). Starting with the walker unit at one end of the track (e.g., pristine 3,4-C_n), cycling between conditions I and II results in some walkers moving from one end of the track to the other (Figure 2). However, this is a consequence of the initial distribution of walker−track conjugates being away from the minimum energy distribution and the system, driven by a gain in entropy, relaxing toward it. Because the steady states correspond to this minimum energy distribution, the walking sequence is not intrinsically directional (by this we mean that in the internal region of a polymeric track made of alternating benzaldehyde−benzylic disulfide footholds, the walker would move, over several acid−base oscillations, in each direction with equal probability). This may appear counterintuitive in light of the nonsymmetric steady-state distributions (the amount of the 1,2 isomer is not equal to the amount of 3,4) found in systems C_3, C_4, C_5, and C_8 (Table 1). The inequality of the 1,2 and the 3,4 isomers is, however, due to substituent effects, which make the two "terminal" footholds electronically and sterically different from their internal counterparts.

To understand the requirements for directional motion, we can consider a polymeric track based on the current track (Figure 5). Here, there are only two fundamentally different types of macrocycles formed between the walker and the track, one in which the track ether linkage is internal to the macrocycle (shown as "ether-macrocycle" in Figure 5) and one in which the track triazole unit is internal to the macrocycle (shown as "triazole-macrocycle" in Figure 5). Each operation i or ii thermodynamically equilibrates this pair of macrocycles about the pivot (kinetically locked) foot. If the two macrocycles have identical relative thermodynamic stabilities under conditions i and ii, any bias toward one end of the track under condition i will be offset by the opposite directional bias under condition ii ($K_i = K_{ii}$). Net-directionality in the walking can thus only occur when the forward/backward ratio under condition i is different from the backward/forward ratio under condition ii

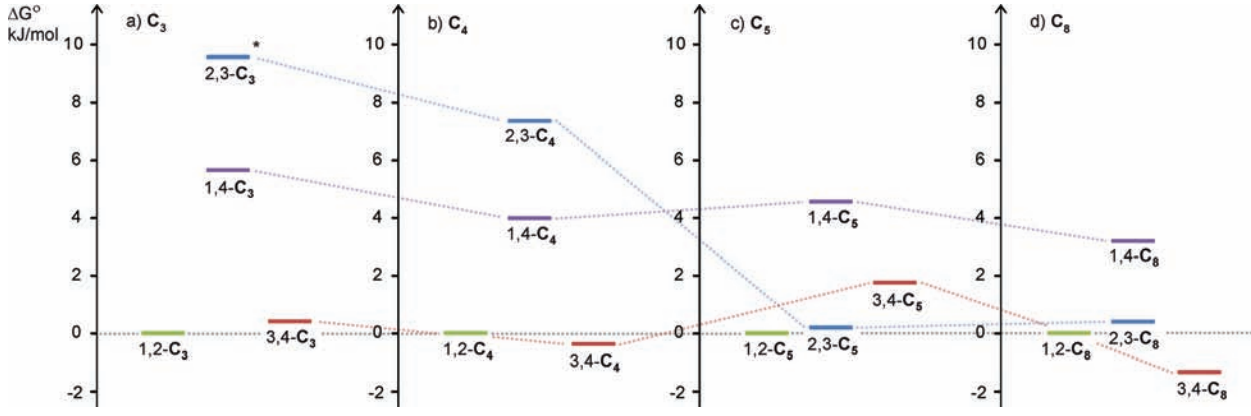

Figure 4. Relative free energies of the four positional isomers of each walker−track conjugate C_n ($n = 3, 4, 5, 8$) determined by the experimental equilibrium ratios between each pair of positional isomers (Scheme 2). The relative energies only apply to the specific reaction conditions (I and II) of the reversible exchange processes ($CHCl_3$, 0.1 mM, room temperature) and should only be considered a qualitative aid for the understanding of ring strain effects within the different compound series. The energies are assumed to be similar in acidic and basic conditions because the product distributions converge to a steady state in Figures 2 and 3 (and section 6 in the Supporting Information) rather than oscillate (which would be the behavior expected if the relative energies change in acid and base). The energy of the 1,2 isomer was set at 0.0 kJ mol^{-1} for each compound series. Dotted lines connect isomers at the same track position. (a) C_3, (b) C_4, (c) C_5, (d) C_8. *The relative free energy shown for 2,3-C_3 is a lower limit value, based on the detection limit of the analytical method (see Scheme 2 caption).

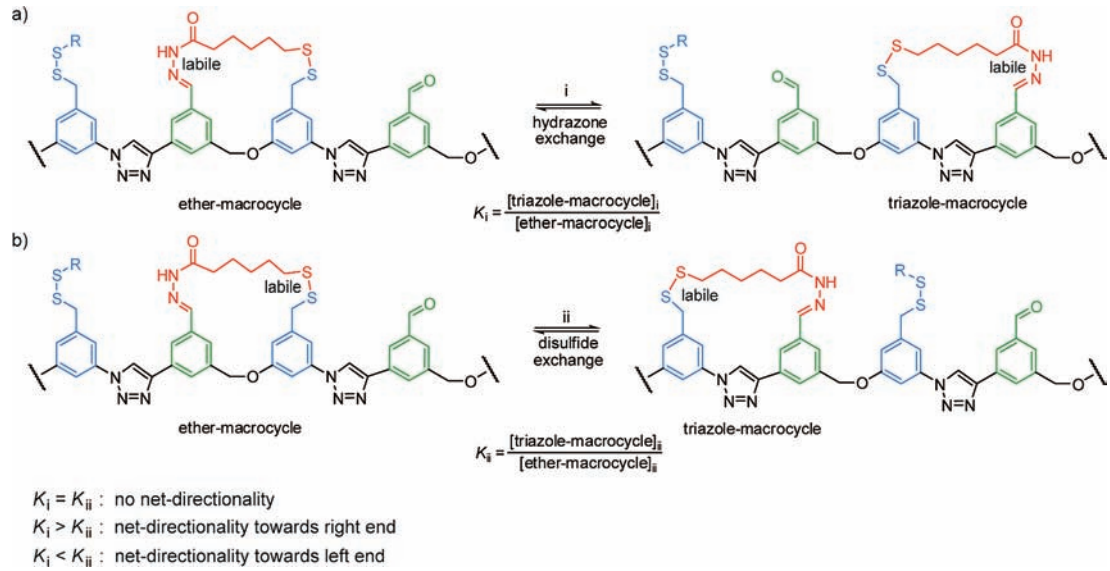

Figure 5. Requirements for directional walker migration along a hypothetical polymeric track based on the $\mathbf{C_5}$ walker−track system. (a) Under conditions i (hydrazone exchange), the walker can pivot at the disulfide foothold and form two different kinds of macrocycles, one incorporating the flexible ether linker (ether-macrocycle) and one incorporating the more rigid triazole linker (triazole-macrocycle). (b) Under conditions ii (disulfide exchange), the walker can pivot about the hydrazone foothold, and the walker can form the same two types of macrocycle with the track. For net-directionality of walker transport, K_i and K_{ii} must have different values.

Scheme 3. Kinetically Controlled Redox Operation for Disulfide Exchange, Illustrated for 2,3-$\mathbf{C}_n$[a]

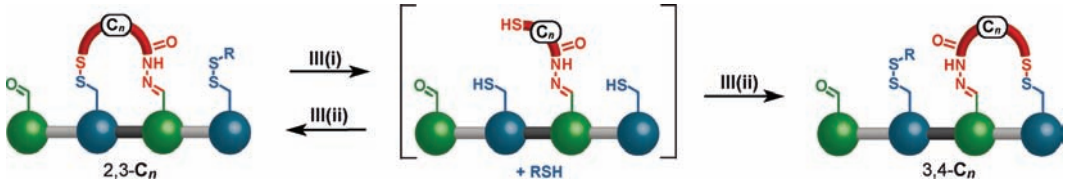

[a] Condition III (i) (reduction of disulfide bonds): 1.0 mM, DTT (6 equiv), DBU (3 equiv), $CDCl_3$, reflux, 2−12 h (progress monitored by ^{1}H NMR). Condition III (ii) (irreversible, oxidative disulfide bond regeneration): 0.1 mM, Et_3N (excess), methyl 3-mercaptopropionate (RSH, 8 equiv), I_2 (ca. 12 equiv), $CDCl_3$/cosolvent, room temperature, 5 min.

($K_i > K_{ii}$ or $K_i < K_{ii}$). If both processes are under thermodynamic control, this will only be the case if the two macrocycles happen to have different relative thermodynamic stabilities under conditions i and ii. We have demonstrated that this is not the case for our walker−track systems using our standard acidic and basic conditions. As a result, net-directional transport cannot be achieved with such systems using only reversible reactions that proceed under thermodynamic control.[41]

One way to overcome this issue is to carry out one of the two exchange processes under kinetic control (Scheme 3). In such a situation, the ratio of positional isomers formed depends on their relative rates of formation, which can differ from their relative thermodynamic stabilities. Under conditions III(i) (1 mM, DTT (6 equiv), DBU (3 equiv), $CDCl_3$, reflux, 2−12 h), the disulfide bonds in 2,3-$\mathbf{C}_n$ can be quantitatively reduced, resulting in a ring-opened intermediate (shown in square brackets in Scheme 3). Rapid oxidation (conditions III(ii), 0.1 mM, Et_3N (excess), $MeO_2CCH_2CH_2SH$ (8 equiv), I_2 (ca.12 equiv), $CDCl_3$/cosolvent, room temperature, 5 min) subsequently regenerates the walker−track disulfide linkages under kinetic control with a different positional isomer ratio to the reversible (thermodynamically controlled) reaction.

The oxidation step for the various walker−track trithiols proceeded efficiently in a variety of solvent systems, and, remarkably, the use of a cosolvent ($CHCl_3$ was kept constant in the 1:1 solvent mixtures) could have a very significant effect on the positional isomer ratio that resulted (Table 2).[42] For example, the oxidation of the $\mathbf{C_5}$ trithiol leads to a 2,3:3,4 ratio of 70:30 in $CHCl_3$:*t*-BuOH (1:1) but a 32:68 ratio; that is, the terminal macrocycle is preferred, in $CHCl_3$:MeOH (1:1). Even highly strained positional isomers (Figure 4) can be accessed using this procedure: although isomer 2,3-$\mathbf{C_3}$ is not detectable in the reaction mixture when 3,4-$\mathbf{C_3}$ is subjected to basic conditions under thermodynamic control (Table 1), the redox reaction under kinetic reaction control using cyclohexane as

(38) These differences are probably a result of insufficient equilibration times (i.e., equilibrium was not reached when the reaction was quenched).

(39) We were also able to simulate "out-of-equilibrium" situations by randomly changing one or more of the four equilibrium ratios that serve as input variables in the spreadsheet program. Thereafter, the ratios do not form a consistent set, and, as a result, the graph does not converge toward a constant composition and instead oscillates indefinitely between two states.

(40) The significant ring strain present in the 2,3 and 1,4 isomers of the $\mathbf{C_3}$ and $\mathbf{C_4}$ systems would make a very lengthy experimental procedure necessary until convergence to the steady states (~15 cycles for $\mathbf{C_3}$ and ~8 cycles for $\mathbf{C_4}$, Table 1).

(41) Directional walking can be achieved solely using reactions that are carried out under thermodynamic control by coupling the stepping processes to energy consumption. For example, in some of the artificial DNA walker systems (refs 16g−i), the "walking" events are reversible, and directionality is achieved by ratchet mechanisms that couple the "walking" equilibria to the consumption of a chemical "fuel".

(42) Other oxidants (e.g., Br_2 and $K_3[Fe(CN)_6]$) were investigated but did not prove superior to I_2 in terms of positional isomer ratios or chemoselectivity.

Table 2. Effect of Cosolvent (1:1 with $CHCl_3$) on the Observed 2,3-$\mathbf{C}_n$:3,4-$\mathbf{C}_n$ Isomer Ratio after Irreversible Oxidation of Trithiol (Compound in Brackets, Scheme 3)[a]

cosolvent	2,3-$\mathbf{C_3}$:3,4-$\mathbf{C_3}$	2,3-$\mathbf{C_4}$:3,4-$\mathbf{C_4}$	2,3-$\mathbf{C_5}$:3,4-$\mathbf{C_5}$
n-hexane	45:55	66:34	65:35
cyclohexane	**47:53**	**65:35**	68:32
Et_2O	40:60	61:39	61:39
MeCN	31:69	49:51	54:46
THF	36:64	58:42	56:44
DMF	20:80	55:45	66:34
MeOH	25:75	36:64	**32:68**
EtOH	35:65	48:52	47:53
i-PrOH	39:61	59:41	54:46
t-BuOH	43:57	62:38	70:30

[a] Pure samples of 3,4-$\mathbf{C}_n$ were submitted to conditions III(i) and III(ii) (see Experimental Section for details). Values are based on HPLC integration and are corrected for the absorbance coefficients at 290 nm (see the Supporting Information).

Table 3. Positional Isomer Distribution during 1.5 Cycles of Biased Operation of $\mathbf{C_5}$ System and Comparison to the Experimentally Observed Minimum Energy Steady-State Distribution a

cycles/conditions	0	0.5/I	1/III	1.5/I	steady-state from conditions I and II (*Table 1*)
1,2-$\mathbf{C_5}$	100%	52%	28%	24%	39%
2,3-$\mathbf{C_5}$	0%	48%	20%	24%	36%
3,4-$\mathbf{C_5}$	0%	0%	28%	**43%**	**19%**
1,4-$\mathbf{C_5}$	0%	0%	24%	9%	6%

[a] See Experimental Section for details on conditions I and III (cosolvent: MeOH). Values are based on HPLC integration and are corrected for the molar absorptivities at 290 nm (see the Supporting Information).

cosolvent affords a 2,3:3,4 ratio of 47:53! Such observations indicated the possibility of obtaining significant directional bias in walker migration by using the irreversible conditions III with an appropriate cosolvent. For the selection of the cosolvent, it is important to consider that the goal of these experiments is to drive the system away from the minimum energy distribution of walkers on the tracks (Table 1). The most promising entries in this respect are cyclohexane for the $\mathbf{C_3}$ and $\mathbf{C_4}$ systems and methanol for the $\mathbf{C_5}$ system (ratios highlighted in Table 2).

Directional Bias of the $\mathbf{C_5}$ System. The effect of introducing the redox conditions III (cosolvent: MeOH) into the walking sequence of the $\mathbf{C_5}$ system is shown in Table 3. In only 1.5 cycles, starting from 100% 1,2-$\mathbf{C_5}$, the walker moves along the track to give 43% 3,4-$\mathbf{C_5}$, as compared to the 19% of 3,4-$\mathbf{C_5}$ present at the steady state using the two sets of reversible conditions (Figure 2 and Table 1). However, further cycles would not increase this directional bias, because each time the reversible conditions I were applied the composition of the mixture would move back toward the minimum energy distribution. When analyzing the origin of the bias toward the right end of the track, it becomes clear that the 1,4-$\mathbf{C_5}$ isomer makes a significant contribution. For example, after cycle 1 (redox step), an unusually high amount of 1,4-$\mathbf{C_5}$ (24%) is present, which in the subsequent step is largely converted to 3,4-$\mathbf{C_5}$.

Directional Bias of the $\mathbf{C_4}$ System. Table 4 shows the effect of introducing the redox conditions III (cosolvent: cyclohexane) into the walking sequence of the $\mathbf{C_4}$ system. Starting from 100% 3,4-$\mathbf{C_4}$, in two cycles the walker moves along the track to give 62% 1,2-$\mathbf{C_4}$, as compared to the 41% present at the steady state using the two sets of reversible conditions (Table 1). It is remarkable to note that using the same reaction sequence (and same track) the $\mathbf{C_5}$ and $\mathbf{C_4}$walkers are transported with biases

Table 4. Positional Isomer Distribution during Two Cycles of Acid−Redox Operation of the $\mathbf{C_4}$ System and Comparison to the Extrapolated Minimum Energy Steady-State Distribution[a]

cycles/conditions	0	0.5/III	1/I	1.5/III	2/I	steady state[b] from conditions I and II
1,2-$\mathbf{C_4}$	0%	0%	58%	46%	**62%**	**41%**
2,3-$\mathbf{C_4}$	0%	63%	4%	25%	5%	3%
3,4-$\mathbf{C_4}$	100%	37%	26%	12%	25%	48%
1,4-$\mathbf{C_4}$	0%	0%	12%	17%	8%	8%

[a] See Experimental Section for details on conditions I and III (cosolvent: cyclohexane). Values are based on HPLC integration and are corrected for the molar absorptivities at 290 nm (see the Supporting Information). [b] Extrapolated from the experimentally determined equilibrium ratio of each pair of positional isomers (Table 1).

Table 5. Positional Isomer Distribution during Two Cycles of Acid−Redox Operation of the $\mathbf{C_3}$ System and Comparison to the Extrapolated Minimum Energy Steady-State Distribution[a]

cycles/conditions	0	0.5/III	1/I	1.5/III	2/I	steady state[b] from conditions I and II
1,2-$\mathbf{C_3}$	0%	0%	41%	38%	**53%**	**52%**
2,3-$\mathbf{C_3}$	0%	44%	~1%	13%	<1%	<1%
3,4-$\mathbf{C_3}$	100%	56%	43%	26%	38%	43%
1,4-$\mathbf{C_3}$	0%	0%	15%	23%	9%	5%

[a] See Experimental Section for details on conditions I and III (cosolvent: cyclohexane). Values are based on HPLC integration and are corrected for the molar absorptivities at 290 nm (see the Supporting Information). [b] Extrapolated from the experimentally determined equilibrium ratio of each pair of positional isomers (Table 1).

to the opposite ends of the track! The oscillating behavior of the composition of the $\mathbf{C_4}$ system under these operating conditions is evident: for example, the amount of 1,2-$\mathbf{C_4}$ present goes from 0%→58%→46%→62%. In this system, the 1,4-$\mathbf{C_4}$ isomer does not contribute to the directional bias. In fact, the high amount of 1,4-$\mathbf{C_4}$ isomer formed during step 3 (cycle 1.5) counteracts the bias toward the left end of the track.

Directional Bias of the $\mathbf{C_2}$, $\mathbf{C_3}$, and $\mathbf{C_8}$ Systems. The relative energies of the various positional isomers in the $\mathbf{C_8}$ system (see Figure 4) suggest that the acid−base and acid−redox operation should give rather similar steady-state values (neither 2,3-$\mathbf{C_8}$ nor 1,4-$\mathbf{C_8}$ are strained enough to give significant directionality by the mechanisms seen for $\mathbf{C_4}$ or $\mathbf{C_5}$, respectively). In the $\mathbf{C_2}$ system, the macrocycle that would incorporate the triazole unit would be so strained that isomer 2,3-$\mathbf{C_2}$ cannot be accessed, even under kinetic control.

Table 5 shows the results obtained when introducing the redox operation III (cosolvent: cyclohexane) into the walking sequence of the $\mathbf{C_3}$ system. Starting from 100% 3,4-$\mathbf{C_3}$, two operational cycles gave 53% 1,2-$\mathbf{C_3}$, a value similar to the 52% present at the steady state for acid−base operations. The lack of directional bias with this walker length is partially due to the lower amount of 2,3-$\mathbf{C_3}$ that can be formed (as compared to the $\mathbf{C_4}$ system), but is mostly a result of the right-end bias contributed by the 1,4-$\mathbf{C_3}$ isomer counterbalancing the left-end bias promoted by the 2,3-$\mathbf{C_3}$ isomer.

The results obtained for the $\mathbf{C_2}$ and $\mathbf{C_3}$ systems indicate that there is a threshold at which ring strain gets too high to allow for the optimum degree of directional bias ($\mathbf{C_3}$), or even for any walker migration to occur via the 2,3 isomer ($\mathbf{C_2}$). However, in case of the $\mathbf{C_3}$ system, it is not only the reduced availability of the 2,3-$\mathbf{C_3}$ isomer under kinetic control (47% formed from 3,4-$\mathbf{C_3}$ as compared to 65% for the 2,3-isomer using the $\mathbf{C_4}$ walker; Table 2) that reduces bias toward the left-end of the

Scheme 4. Crossover Study on the Processivity of the $\mathbf{C_5}$ System[a]

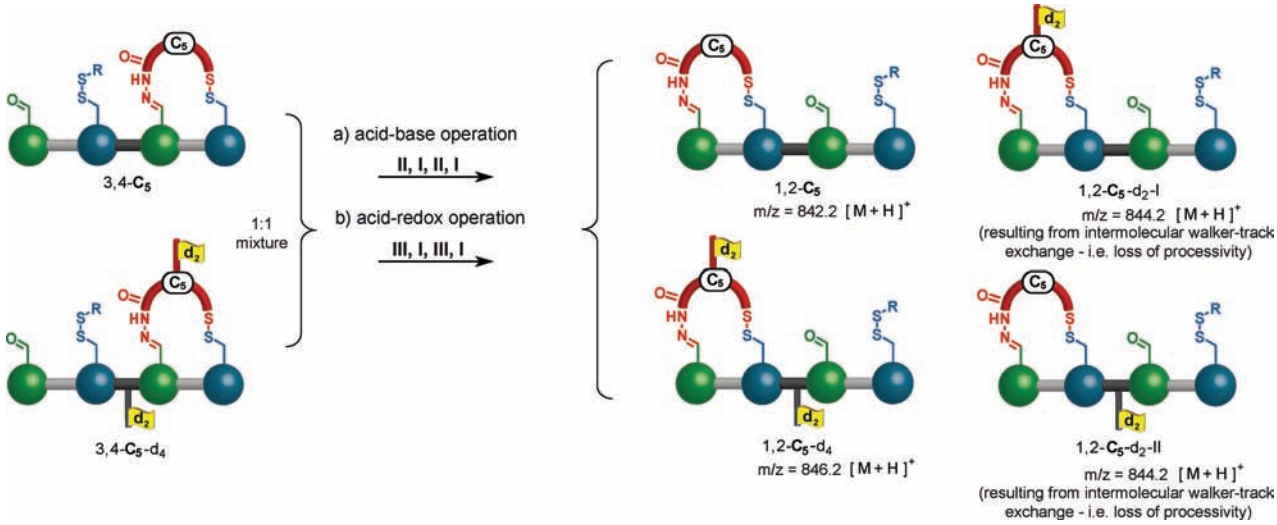

[a] Condition I (reversible hydrazone exchange): 0.1 mM, TFA, $CHCl_3$, room temperature, 6−96 h (monitored by HPLC until the distribution no longer changed). Condition II (reversible disulfide exchange): 0.1 mM, DTT (10 equiv), DBU (40 equiv), dimethyl 3,3′-disulfanediyldipropanoate (20 equiv), $CHCl_3$, room temperature, 12−48 h (monitored by HPLC until the distribution no longer changed). Condition III (i) (reduction of disulfide bonds): 1.0 mM, DTT (6 equiv), DBU (3 equiv), $CDCl_3$, reflux, 2−12 h (progress monitored by ^{1}H NMR). Condition III (ii) (irreversible, oxidative disulfide bond regeneration): 0.1 mM, Et_3N (excess), methyl 3-mercaptopropionate (RSH, 8 equiv), I_2 (ca. 12 equiv), $CDCl_3$/MeOH, room temperature, 5 min.

track, but also the fact that the 1,4-$\mathbf{C_3}$ isomer favors transport in the opposite direction. The small energy differences between the various positional isomers of the $\mathbf{C_8}$ system (Figure 4) suggest that there is also an upper limit to the walker length after which ring strain becomes too low to bias directionality effectively. Interestingly, ring strain has been identified as a key feature thought to generate the directional bias in kinesin[43] and myosin-V.[44]

Determining the Processivity of Walking in the $\mathbf{C_5}$ Walker−Track System. The processivity of the acid−base and acid−redox walking experiments of the $\mathbf{C_5}$ system was determined by double-labeling crossover experiments (see the Supporting Information for details). The double-labeled walker−track conjugate 3,4-$\mathbf{C_5}$-d_4 (Scheme 1c) was mixed with an unlabeled sample of 3,4-$\mathbf{C_5}$ in a 1:1 ratio (Scheme 4). This mixture was subjected to either the acid−base walking cycle conditions (Scheme 4a) or the acid−redox walking cycle conditions (Scheme 4b). The product distribution of both experiments was analyzed by HPLC−MS (high performance liquid chromatography−mass spectrometry).[45]

The results of these two experiments are shown in Figure 6. The blue bars represent the experimentally obtained isotopic distribution of the sample before operation, while the green bars represent the theoretical isotopic distribution that would be expected if full statistical scrambling (intermolecular exchange of the walker molecules with the tracks) had occurred. The red bars show the experimentally obtained isotopic distribution after operation (Figure 6a for two acid−base cycles; Figure 6b for two acid−redox cycles).

The arrows indicate the *m*/*z* value of single-labeled species, which are indicators of a loss of processivity during the migration of the walker along the track (Scheme 4). The difference between the nondirectionally biased (acid−base) and directionally biased (acid−redox) operations is evident, with the former exhibiting a significantly higher level of processivity after four operational steps. Mathematical analysis (see the Supporting Information) gives a mean step number[46] of 37 for acid−base operation, whereas using acid−redox cycles the

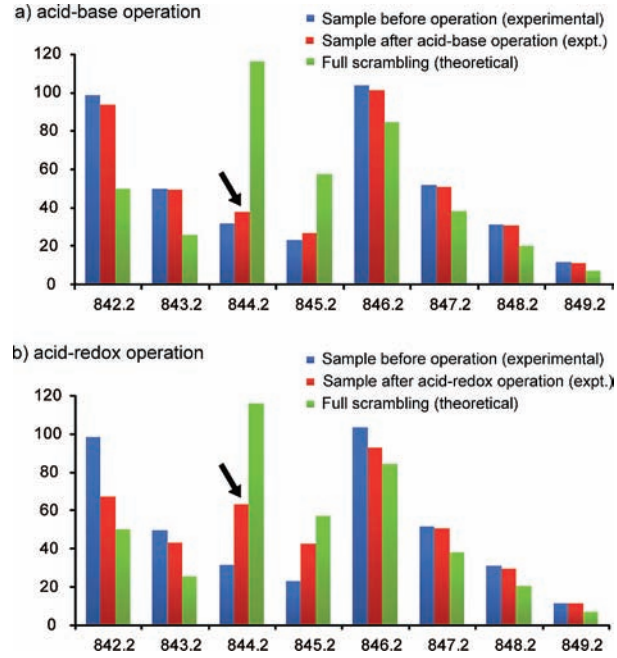

Figure 6. Results of the crossover study on the processivity of the $\mathbf{C_5}$ system: (a) acid−base operation over two cycles; (b) acid−redox operation over two cycles (see Scheme 4). Shown are the (normalized) isotopic distributions of the 1:1 mixture before operation (blue; experimental), after operation (red; experimental), and the distribution that would be expected when full statistical scrambling occurred (green; theoretical). The distribution (red bars and blue bars) of experimental data points is the average of 10 runs for each experiment. This procedure demonstrated the reproducibility of the mass spectrometry data and enabled the isotope scrambling to be analyzed for statistical significance (see the Supporting Information).

(43) (a) Hyeon, C.; Onuchic, J. N. *Proc. Natl. Acad. Sci. U.S.A.* **2007**, *104*, 2175–2180. (b) Yildiz, A.; Tomishige, M.; Gennerich, A.; Vale, R. D. *Cell* **2008**, *134*, 1030–1041. (c) Cochran, J. C.; Kull, F. J. *Cell* **2008**, *134*, 918–919.

(44) (a) Veigel, C.; Schmitz, S.; Wang, F.; Sellers, J. R. *Nat. Cell Biol.* **2005**, *7*, 861–869. (b) Trybus, K. M. *Nat. Cell Biol.* **2005**, *7*, 854–856.

(45) The product mixtures were not purified by HPLC. All oligomers and other side-products were retained in the sample.

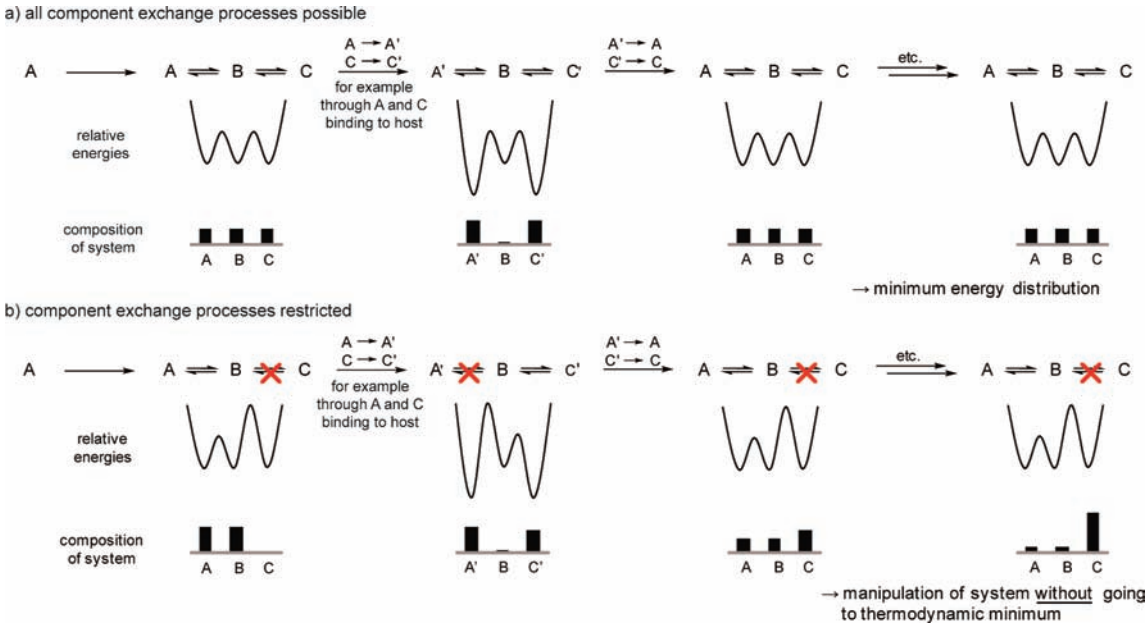

Figure 7. Ratchet mechanisms and systems chemistry: the potential utility of restricted component exchange processes. (a) Chemical system of three components (A, B, and C) at equilibrium. Repeated manipulation (through host binding event (A→A′, C→C′)) does not lead away from thermodynamic minimum. (b) Chemical system of three components (A, B, and C) with restricted component exchange processes (an energy ratchet mechanism). Repeated manipulation shifts the composition away from thermodynamic minimum.

walker takes an average of seven steps before detaching. In comparison, wild-type kinesins have a mean step number of 75−175 with an average run length of ∼1 μm.[12]

The loss of processivity during the reactions under thermodynamic control (acid and base catalyzed cycles) is most likely a result of the formation of oligomers in which a walker moiety bridges two tracks and, after the following operational step (which breaks one of the walker−track bonds), is no longer located on its original track (see the Supporting Information, Scheme S4b). Loss of processivity via complete detachment of the walker moiety can be excluded for two reasons: (i) Starting from one pristine isomer, only mixtures of two isomers, never all four, are ever observed (Scheme 2; see, for example, the first half-cycle in Figure 2); and (ii) under any of the operating conditions, we never detected[47] a detached walker moiety, bare track, or track with two walker moieties.

The higher loss of processivity during the kinetically controlled step probably results from the formation of intramolecular disulfide bonds between the sulfur groups on the track, the sulfur group of the walker forming a disulfide with the placeholder group, which causes the walker to detach from the track during the subsequent acidic step. Indeed, HPLC analysis of the redox step showed the appearance of oligomers and two monomeric side products that do not occur during the thermodynamically controlled disulfide exchange (see the Supporting Information, Scheme S4c).

Relating Molecular Walkers to Systems Chemistry. Motors and machines at the molecular level operate by chemical laws and statistical mechanisms, not the Newtonian laws for momentum and inertia that determine the mechanisms of mechanical machines in the macroscopic world.[2,13a] The manipulation of the statistical distribution of the molecular walkers presented in this Article can be seen as a new facet of synthetic systems chemistry.[48] In most of the mixtures studied to date from the point of view of systems chemistry,[49] each molecular component is in equilibrium with all the other components. In the walker systems presented here, however, only subsets of the four positional isomers (1,2-$\mathbf{C}_n$, 2,3-$\mathbf{C}_n$, 3,4-$\mathbf{C}_n$, and 1,4-$\mathbf{C}_n$) can exchange with each other under any given set of conditions. This restriction of the component exchange processes is a fundamental property that can be exploited in a mechanism (a ratchet mechanism[2]) to drive the system away from the thermodynamic minimum energy distribution of the components.

Such behavior is illustrated in Figure 7 for a system of three components A, B, and C in which both the relative depths of the energy minima can be varied (e.g., A and C can bind to a host molecule, decreasing their relative free energy (A→A′ and C →C′ in Figure 7) and, in Figure 7b only, the relative heights of the energy maxima can be varied (e.g., if A exchanges only with B under conditions in which B does not exchange with C).

If all three components are in equilibrium (Figure 7a), the addition of the host leads to a new distribution (with A′ and C′ being the major components) corresponding to the new thermodynamic minimum of the system; that is, the composition of the system is a function of the relative free energies of the three components. Removal of the host molecule leads back to the original distribution. Such a manipulation, even when repeated, cannot result in an out-of-equilibrium state of the system.

(46) The mean step number describes the number of operational steps after which one-half of the molecules have lost processivity (i.e., have detached or exchanged with others in the bulk).
(47) No peaks with these *m*/*z* values were detected by HPLC−MS.

(48) (a) Ludlow, R. F.; Otto, S. *Chem. Soc. Rev.* **2008**, *37*, 101–108. (b) Nitschke, J. R. *Nature* **2009**, *462*, 736–738.
(49) For examples, see: (a) Grote, Z.; Scopelliti, R.; Severin, K. *Angew. Chem., Int. Ed.* **2003**, *42*, 3821–3825. (b) Buryak, A.; Severin, K. *Angew. Chem., Int. Ed.* **2005**, *44*, 7935–7938. (c) Chung, M.-K.; Hebling, C.; Jorgenson, J.; Severin, K.; Lee, S. J.; Gagné, M. R. *J. Am. Chem. Soc.* **2008**, *130*, 11819–11827. (d) Ludlow, R. F.; Otto, S. *J. Am. Chem. Soc.* **2008**, *130*, 12218–12219. (e) Sarma, R. J.; Nitschke, J. R. *Angew. Chem., Int. Ed.* **2008**, *47*, 377–380. (f) Ludlow, R. F.; Otto, S. *J. Am. Chem. Soc.* **2010**, *132*, 5984–5986. (g) Mal, P.; Nitschke, J. R. *Chem. Commun.* **2010**, *46*, 2417–2419. (h) Campbell, V. E.; de Hatten, X.; Delsuc, N.; Kauffmann, B.; Huc, I.; Nitschke, J. R. *Nat. Chem.* **2010**, *2*, 684.

If only one of the two exchange processes is possible under any one set of conditions, however, the composition of the system can be moved away from the thermodynamic minimum (Figure 7b). Repetitive addition and removal of the host, while switching between the pairs of components that are able to exchange, leads to a composition that is far away from the thermodynamic minimum (right-hand side of Figure 7b). Such a concerted manipulation of the thermodynamics and kinetics of a system corresponds to a flashing energy ratchet mechanism.[2,3e,13a] The mutually exclusive conditions available for hydrazone and thiol/disulfide exchange[24b−d] represent an appealing opportunity for the manipulation of out-of-equilibrium chemical systems, as well as ratcheted machine mechanisms,[2,13a] through such concepts.

Conclusions

We have described five small-molecule systems in which a molecular walker with chemical "legs" of varying length moves up and down a four-foothold track primarily through a passing-leg gait mechanism. Repetitive switching of fully reversible walking operations does not lead to intrinsically directional migration of the walker units, but to a minimum energy distribution of walkers on the tracks. Directionality of the walking sequence can, however, be achieved for two of the five systems studied by replacing one of the reversible reactions with a kinetically controlled redox operation, the outcome of which can be significantly manipulated by addition of a cosolvent. The length of the spacer unit between the walker feet is crucial for generating ring strain with the track necessary for maximizing directional bias. A crossover isotopic labeling study shows that directionality gained by introducing the kinetically controlled redox step comes at the price of reduced processivity (mean step number 7, as compared to 37 under acid−base conditions). Although they are extremely rudimentary systems, the $\mathbf{C_4}$ and $\mathbf{C_5}$ walker−track conjugates exhibit four of the essential characteristics of linear molecular motor dynamics: processive, directional, repetitive, and progressive migration of a molecular unit up and down a molecular track. Improvements to these first generation designs are required to address problems associated with folding (which generates the "double step" 1,4-isomer), reaction time scales (currently several hours for each operation), oligomer formation (which results in reduced processivity), chemoselectivity, and improved (ratchet) mechanisms[50] for directional bias. Such systems, as well as extended tracks and walkers that can capture and release cargoes, are currently under investigation in our laboratory.

Experimental Section

General Procedure for Acid-Catalyzed Hydrazone Exchange (I). To a 0.1 mM solution of 1,2-$\mathbf{C}_n$ (typically 1 mg in ca. 10 mL; 1.0 equiv) in $CHCl_3$ (HPLC grade) was added 5 drops of a solution of 20% v/v TFA (CF_3CO_2H) and 1% v/v H_2O in $CHCl_3$ (HPLC grade). The mixture was stirred at room temperature, and the progress of the equilibration was followed by analytical HPLC (see the Supporting Information). When the relative ratios of the isomers were stable (generally 6−96 h), the mixture was washed with an aqueous solution of $NaHCO_3$. The layers were partitioned, and the aqueous layer was extracted with $CHCl_3$. The combined organic layers were dried over $MgSO_4$. The solvents were removed under reduced pressure, and the amount and constitution of the mixture were determined by weight and, after dissolving in a defined amount of $CHCl_3$, analytical HPLC.

General Procedure for Base-Catalyzed Disulfide Exchange (II). To a 0.1 mM solution of 3,4-$\mathbf{C}_n$ (typically 1 mg in 10 mL; 1.0 equiv) in $CHCl_3$ (HPLC grade) were added DBU (40 equiv), DTT (10 equiv), and dimethyl 3,3′-disulfanediyldipropanoate (20 equiv) from stock solutions. The mixture was stirred at room temperature, and the progress of the equilibration was followed by analytical HPLC. When the relative ratios of the isomers were stable (generally 12−48 h), the excess of DTT was oxidized by dropwise addition of a solution of I_2 in $CHCl_3$ until a slight brown color persisted. An aqueous solution of NH_4Cl and Na_2SO_3 was added, and the mixture was stirred vigorously until decolorization was complete. The layers were partitioned, and the aqueous layer was extracted with $CHCl_3$. The combined organic layers were dried over $MgSO_4$. After workup, the product distribution (free of DTT and DBU) was no longer dynamic, and the solvent could be removed to allow analysis by weight and analytical HPLC (see the Supporting Information).

General Procedure for Redox-Mediated Disulfide Exchange (III). (i) Reduction step: DTT (6 equiv) and DBU (3 equiv) were added from stock solutions to a 1 mM solution of 2,3-$\mathbf{C}_n$ (1 equiv) in $CDCl_3$ or $CHCl_3$. The mixture was heated under reflux until ^1H NMR showed that all disulfide bonds had been reduced (2−12 h).

(ii) Oxidation step: The above solution was diluted to 0.1 mM with a 1:1 mixture of $CHCl_3$ and cosolvent (MeOH for $\mathbf{C_5}$, cyclohexane for $\mathbf{C_3}$ and $\mathbf{C_4}$). Et_3N (5 drops) and methyl 3-mercaptopropionate (8 equiv) were added. At room temperature, a solution of I_2 in $CHCl_3$ was added to the mixture until the brown color persisted. An aqueous solution of NH_4Cl and Na_2SO_3 was added, and the solution was stirred vigorously until decolorization was complete. The layers were partitioned, and the aqueous layer was extracted with $CHCl_3$. The combined organic layers were dried over $MgSO_4$. For the $\mathbf{C_5}$ system, at this stage a broad-window preparative HPLC was carried out (see reference A for details) to remove excess reagents, waste products, and other impurities (the two-step redox sequence produces more byproducts than the acid or base catalyzed procedures). This purification step was omitted for the processivity study ($\mathbf{C_5}$) and for the operation of the $\mathbf{C_3}$ and $\mathbf{C_4}$ systems.

Note: The molar ratios of DBU and DTT used during the base-catalyzed disulfide exchange experiments (40 and 10 equiv, respectively) are higher than those used during the reduction step of the redox disulfide exchange experiments (3 and 6 equiv, respectively) because there is a 10-fold difference in concentration at which the experiments were carried out (0.1 and 1.0 mM, respectively). The DBU:DTT ratio is also reversed (from 4:1 to 1:2) in the two experiments. The rationale behind these changes reflects the different objectives of the two types of exchange experiments: During the base-catalyzed exchange experiment, DTT is added to increase the rate of disulfide exchange for which thiolates are a necessary intermediate; during the redox operation, the excess DTT results in quantitative reduction of the disulfide bonds. The resulting thiols are subsequently rapidly oxidized by iodine to affect a kinetically controlled reaction outcome.

Acknowledgment. We thank the EPSRC National Mass Spectrometry Service Centre (Swansea, UK) for high resolution mass spectrometry. This research was funded through the European Research Council Advanced Grant WalkingMols. D.A.L. is an EPSRC Senior Research Fellow and holds a Royal Society-Wolfson Research Merit Award.

Supporting Information Available: Full experimental procedures for the synthesis of compounds 3,4-$\mathbf{C_2}$, 3,4-$\mathbf{C_3}$, 3,4-$\mathbf{C_4}$, and 3,4-$\mathbf{C_8}$, HPLC traces for $\mathbf{C_3}$ and $\mathbf{C_4}$, detailed information on the processivity study, and extrapolation graphs. This material is available free of charge via the Internet at http://pubs.acs.org.

JA106486B

(50) For a small molecule that can walk in either direction along a track through a light-driven energy ratchet mechanism, see: Barrell, M. J.; Campaña, A. G.; von Delius, M.; Geertsema, E. M.; Leigh, D. A. *Angew. Chem., Int. Ed.* **2010**, *49*. DOI: 10.1002/anie.201004779.